

FUZZY TECHNIQUES IN THE FUNCTIONAL APPROXIMATION OF VOLUMETRIC CAPNOGRAMS

Adriana G. Scandurra¹, Ana L. Dai Pra¹, Lucía I. Passoni¹,
Gustavo J. Meschino¹, Fernando M. Clara¹, Gerardo Tusman²,
Stephan H. Böhm³

¹Laboratorio de Bioingeniería, Departamento de Electrónica,
Facultad de Ingeniería, Universidad Nacional de Mar del Plata,
Mar del Plata, Argentina
scandu@fi.mdp.edu.ar

²Departamento de Anestesiología, Hospital Privado de Comunidad
Mar del Plata, Argentina

³Research Centre for Nanomedicine,
Centre Suisse d'Electronique et de Microtechnique SA
Landquart, Switzerland

Abstract

The Volumetric Capnography (VC) is the plot of amounts of expired CO₂ within one tidal breath. The estimation of physiologic parameters derived from the VC is useful in the study of respiratory physiology, clinical anesthesia and critical care medicine. In this work we propose the use of a function based on a Takagi-Sugeno fuzzy model and a functional approximation based on the Levenberg-Marquardt algorithm to approximate the VC, with the goal to compute two variables of interest: the airway dead space (V_{Daw}) and the slope of the so-called Phase III (S_{III}). These models presented a good performance in those capnograms that showed difficulties to be modeled with traditional medical analysis.

Key words: volumetric capnography, Takagi-Sugeno Fuzzy Inference Systems, functional modeling.

1 Introduction

The Volumetric Capnography (VC) is a plot of the CO₂ elimination vs. the expired volume. The estimation of derived physiologic parameters of VC is relevant in the study of respiratory physiology, clinical anesthesia and critical care medicine [7, 9] The shape of the VC provides important clinical informa-

tion because it is characteristically modified by chronic diseases such as chronic obstructive pulmonary disease (COPD) or emphysema, and acute events such as pulmonary embolism and asthma.

Most approaches to studying VC curves are based on their geometrical analysis. Ward S. Fowler, who is one of the first researchers in the field, originally applied his method by hand, a subjective technique to be used at the bedside [4]. Different researchers have adapted Fowler's method and they have described other techniques for VC analysis to be implemented in computational algorithms in order to make VC useful in the clinical field [3, 11]. One key target of all techniques is the adequate determination of the position of several significant points in the VC. Such points are very sensitive to changes in the morphology of the curve and they are susceptible to the acquisition noise.

The purpose of this study is to find an adequate functional approximation of the VC, from which specific points of interest can then be accurately and dynamically computed.

We present three models based on Takagi-Sugeno fuzzy techniques [1, 13] and a fourth model which is a functional approximation by means of the Levenberg-Marquardt algorithm [10].

The functional approximation of each VC is obtained from a fuzzy architecture, achieving less susceptibility to noise, and obtaining more accuracy in determining points of interest in hard VCs, comparing with the results of the traditional medical analysis.

1.1 Volumetric Capnogram Analysis

A typical VC curve is shown in Fig.1, where three phases are observed. Phase I is the portion of the tidal volume free of CO_2 at the beginning of expiration. Phase II consists of a rapid S-shaped rise, being the result of mixing of dead-space gas and alveolar gas. Finally, Phase III (alveolar plateau) represents the CO_2 -rich gas coming from the alveoli.

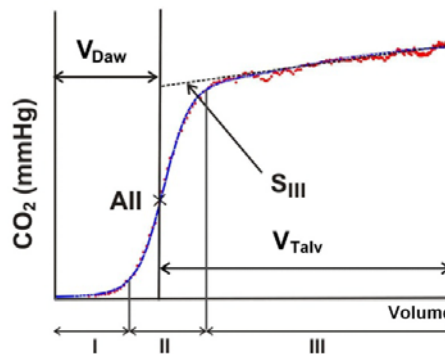


Figure 1. Phases of VC

Most approaches for parameterization of the VC curves are based on geometric analysis. The pursued goal is the adequate determination of the “airway-alveolar” interface position (*AII*); i.e. the boundary between the airway dead-space (V_{Daw}) and alveolar tidal volume (V_{Tav}) regions. This interface sets the boundary between convective and diffusive transport of CO_2 within the lungs [2]. The precise definition of the *AII* is mandatory for the accurate computation of the VC derived variables [10]. Besides, another important derived variable from VC is the slope of Phase III (S_{III}), because this slope depends directly on the distribution of ventilation and perfusion within the lungs.

2 Methods

The Fowler and functional approximation methods were applied to obtain the values of derived variables of VC defined in section 1.1.

2.1 Fowler’s method

The Fowler method consists of the following sequential steps (Fig. 2): First, S_{III} is computed by linear regression using a fixed portion of the VC data between 40 and 80% of the expired volume. Secondly, the position of *AII* is searched by iteratively moving a vertical line between the start of phase II and its boundary towards the right so that in the end, the areas “*p*” and “*q*” became equal. V_{Daw} is the abscisa value (volume) at the point *AII*.

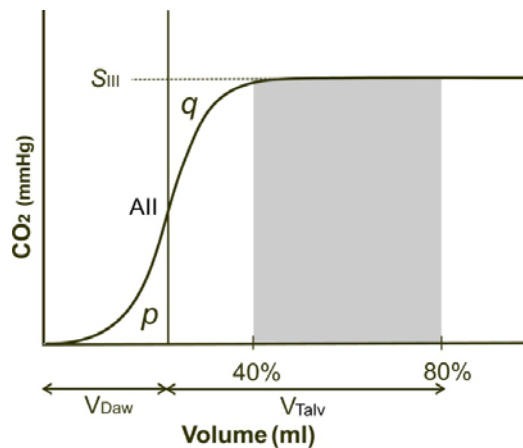


Figure 2. Fowler “equal area” method ($p = q$)

2.2 Functional approximation methods

Four models are proposed to generate analytic functions in order to fit each VC data (f_{VC}). The first model, FA-LMA (Functional Approximation with Levenberg-Marquardt algorithm) is an optimization of a function created *ad-hoc* for this problem [6] (see Appendix A). The other three models are based on first order Takagi-Sugeno Fuzzy Inference Systems (TS) (see Appendix B) [8]. For each TS model the rules are generated in three different ways:

- by grouping the input-output data using subtractive clustering [12]. Symmetrical Gaussian functions are used as membership functions (M1).
- by using subtractive clustering, and then optimized with an ANFIS model (Adaptive Neuro-Fuzzy Inference System) [5, 6]. The membership functions are defined as the product of two sigmoid functions (M2). These functions have four parameters to be adjusted.
- by using grid partition method, and then optimized with an ANFIS model (M3). The same membership functions as in the M2 model are used.

In the M_1 model the membership function is:

$$\mu(x) = e^{\frac{-(x-c)^2}{2\sigma^2}}, \quad (1)$$

where c and σ are the parameters of a gaussian function. The gaussian functions were selected because of their smoothness, given that they were more adequate to model the cuasi-sigmoidal VC shape.

To increment the freedom degrees when adapting with the ANFIS model we propose the use of the product of two gaussian as membership function that shows four parameters to be adjusted.

In the M_2 and M_3 models the membership function is:

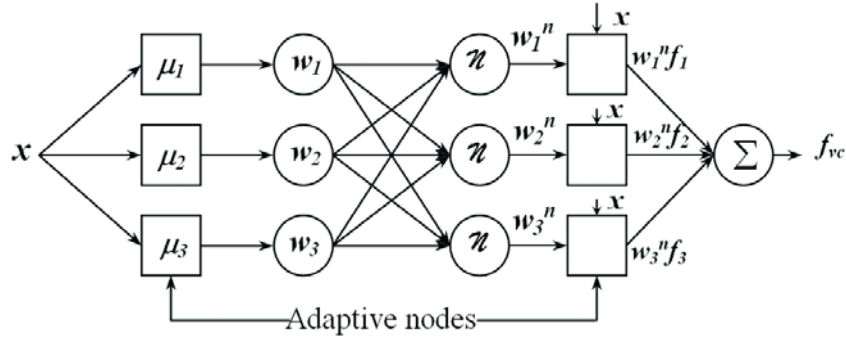
$$\mu(x) = g_1(x) * g_2(x), \quad (2)$$

where:

$$g(x) = \frac{1}{1 + e^{-\alpha(x-c)}}, \quad (3)$$

α and c are the parameters of a sigmoid function.

The ANFIS model architecture is:



Where μ_i are the membership functions.

$$\mathcal{N} \rightarrow w_i^n = \frac{w_i}{w_1 + w_2 + w_3} \quad f_i = a_i x + b_i \quad f_{vc} = \sum_{i=1}^3 f_i w_i^n \quad (4)$$

The training method of the ANFIS is a combination of least-squares estimation with the backpropagation algorithm.

Once the analytic function f_{vc} is obtained, the derived variables are calculated. The point *AII* is mathematically determined as the inflection point of the whole f_{vc} , being V_{Daw} the abscisa value (volume) of *AII*.

The phase III is defined (see Fig.1 and Fig.3) as starting at the point *B*, the right hand maximum of the 3rd derivative of f_{vc} . Since it is of interest to find the slope of the phase III, this phase was divided in thirds, and the middle one is selected for being less influenced by the curve between phase II and phase III. This third was divided into ten equidistant points and f_{vc} slopes (1st derivatives) in these points were computed. The mean value of such ten slope values determines S_{III} .

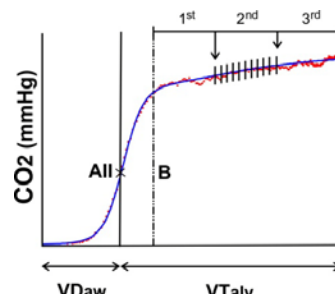


Figure 3. VC-derived variables using the analytic function (see the text for more details)

In order to compare the computational efficiencies of the approximations we measured the computational time to obtain the analytic function (*CTF*), the computational time to get the VC derived variables (*CTDV*) and also we computed the mean square error of the approximation (*MSE*).

3 Materials

The performance of the TS models and FA-LMA model are compared among them in order to assess their effectiveness in uneven VCs. With this purpose in mind, an expert in anesthesiology and respiratory physiology selected three particular VCs (VC_1 , VC_2 and VC_3):

- VC_1 is a typical record with little noise in the phase III, which is approximately linear.
- VC_2 is a record with a “jump” between phases I and II, without excessive noise in this phase and phase III showing a curve shape.
- VC_3 is similar to the previous record, but it has no “jumps” and at the same time it is noisier in the phase II.

A total of 100 VCs from 10 patients undergoing general anesthesia were analyzed to test the TS's and FA-LMA models.

After approval by the local Ethics Committee and having the written informed patients' consents, we enrolled 10 mechanically ventilated ASA I-II patients undergoing general anesthesia, aged 40-70 years. Standard monitoring includes ECG, pulse oxymetry, noninvasive arterial pressure and capnography. Anesthesia was induced with propofol 1.5-2 mg kg⁻¹, fentanyl 5 µg kg⁻¹ and vecuronium 0.08 mg kg⁻¹ and maintained with a continuous infusion of propofol 100 µg kg min and remifentanyl 0.5 µg kg min. Lungs were ventilated through a cuffed endotracheal tube with an Avance Workstation (GE, Madison, WI, USA) using the following settings: tidal volume of 8 ml kg⁻¹, respiratory rate of 15 bpm, inspiration to expiration ratio of 1:2 without inspiratory pause and FiO₂ of 0.5.

Data on VC and respiratory mechanics were recorded continuously and on a breath-by-breath basis using the NICO capnograph connected to a laptop and specific software DataColl (Respironics, Wallingford, Conn., USA). The mainstream sensor was placed between the endotracheal tube and the “Y” piece of the anesthesia circuit. The response time of the CO₂ sensor was < 60 ms and the resolution was 2 mmHg. The fixed orifice differential pressure flow sensor with a measurement range between 1 and 180 L/min had an accuracy of 3%. Calibration was performed according to manufacturer's guides.

3 Results

The comparison of the performance among M_1 , M_2 , M_3 and FA-LMA models, using previously defined indexes and VCs, is shown at Table 1, Table 2 and Table 3. The computations were performed using Matlab® software running in a PC with an AMD Athlon® 64 X2 Dual Core Processor 4000, 2.11 Ghz, 1 Gb Ram.

Table 1: Comparison of performance indexes among the three TS models (M_1 , M_2 and M_3) and FA-LMA model.
CTF: computation time of the analytic function.

<i>Model</i>	<i>CTF [s]</i>		
	<i>VC₁</i>	<i>VC₂</i>	<i>VC₃</i>
M_1	0.598	0.592	0.569
M_2	0.761	0.799	0.772
M_3	0.598	0.636	0.615
FA-LMA	0.754	0.868	0.824

Table 2: Comparison of performance indexes among the three TS models (M_1 , M_2 and M_3) and FA-LMA model.
CTDV: computation time of the derived variables of interest.

<i>Model</i>	<i>CTDV [s]</i>		
	<i>VC₁</i>	<i>VC₂</i>	<i>VC₃</i>
M_1	25.64	29.12	28.93
M_2	70.29	79.57	79.71
M_3	70.07	80.53	81.15
FA-LMA	3.364	3.775	3.788

Table 3: Comparison of performance indexes among the three TS models (M_1 , M_2 and M_3) and FA-LMA model.
MSE: mean square error of the approximation.

<i>Model</i>	<i>MSE</i>		
	<i>VC₁</i>	<i>VC₂</i>	<i>VC₃</i>
M_1	0.724	0.523	0.332
M_2	0.423	0.224	0.307
M_3	0.344	0.247	0.274
FA-LMA	0.376	0.926	0.582

Figure 4 shows the VC raw data (red points) and the obtained functions using the four models (blue lines). Columns 1, 2 and 3 show the results for VC_1 , VC_2 and VC_3 respectively obtained by the four models: M_1 , M_2 , M_3 and FA-LMA (one row per model).

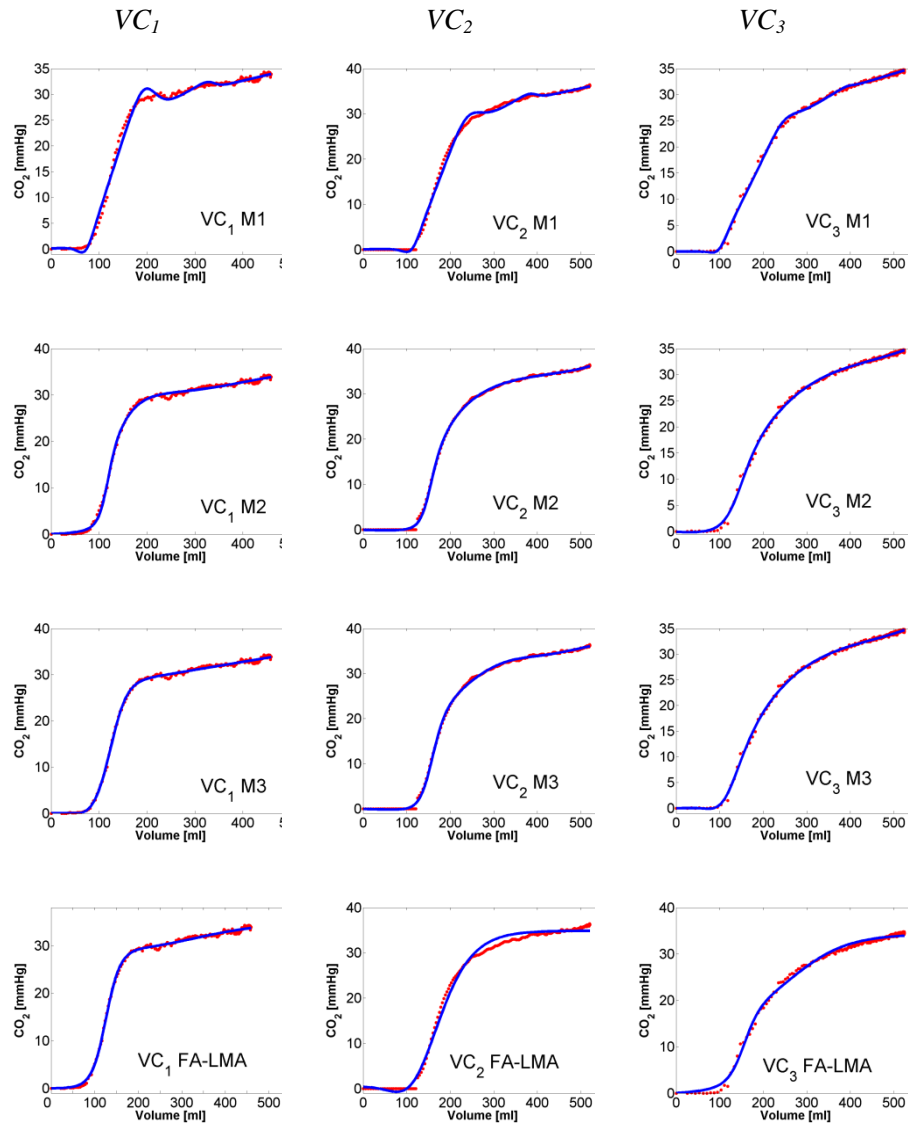


Figure 4. VC raw data (red points) and obtained functions using the proposed models (blue lines) for the selected VCs

Figures 5, 6 and 7 show the final membership functions belonging to M_1 , M_2 and M_3 at the modeling of VC_3 .

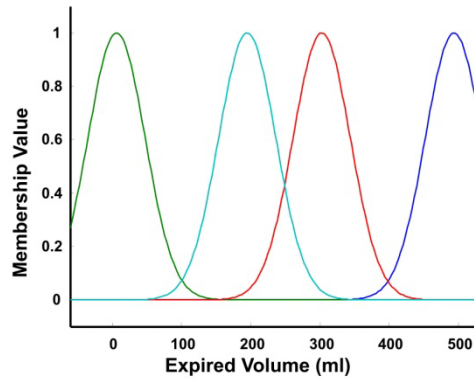


Figure 5. Membership functions of M_1 model

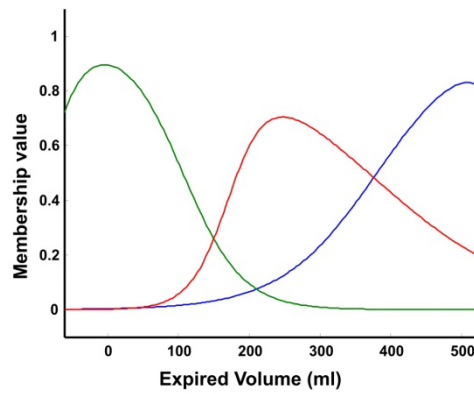


Figure 6. Membership functions of M_2 model

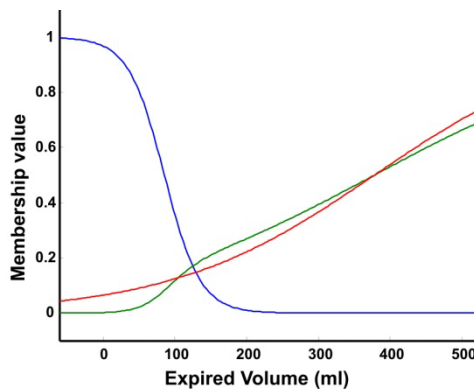


Figure 7. Membership functions of M_3 model

As the main objective in this work is to fit each VC, then the MSE index is selected to evaluate the performance of the model. The M_3 model showed the best performance among the TS models according to the MSE index. As a result, it was selected to be compared against classical models. The coefficient of variation was selected as a quality index of derived variables of interest (V_{Daw} and S_{III}), because the inter- and intra-patient variability do not allow a direct comparison among their values.

Table 4 shows the mean values of MSE and the coefficient of variation of the 100 VC.

Table 4. Comparison of MSE and coefficient of variation values obtained with M_3 and FA-LMA models.

Model	MSE	Coefficient of variation	
		V_{Daw}	S_{III}
M_3	0.3106 ± 0.0889	0.0095	0.011
FA-LMA	0.5865 ± 0.2166	0.0381	0.039

4 Conclusions

One of the limitations of studies that compare methodologies for VC analysis is the lack of an accepted gold standard. Ward S. Fowler was the first to describe a technique for such an analysis and it has been commonly used as the reference method. One important methodological limitation of Fowler’s method is that the computation of V_{Daw} depends on a prior determination of S_{III} . Therefore, Fowler’s technique could be influenced by a “contamination” resulting from sequential and cumulative errors [10]. This is not the case for the TS and FA-LMA models because measurements of V_{Daw} as well as most of the derived variables of VC are computed independently using the analytic function.

The FA-LMA model requires a previously defined *ad-hoc* function whose parameters must be adjusted, while in M_3 , both the function and its parameters are automatically generated by the model. Based on the analysis of MSE and coefficient of variation, the M_3 model, compared to the FA-LMA model, shows less susceptibility to noise, and it presents more precision in determining the airway-alveolar interface, airway dead space and slope of phase III. This dynamically adaptive M_3 model is mathematically robust, and thus suitable for computing the derived variables from clinical VC deformed by pathologies.

Appendix A

The VC is an asymmetrical sigmoid curve that can be represented by a mathematical function. This continuous real-valued function is obtained by a non-linear least square curve fitting, which can be viewed as an optimization problem of the parameters of a proposed function (model function), as Equation (5). Figure 8 shows this model function.

$$f(t, \mathbf{x}) = f_0(t, \mathbf{x}) + f_1(t, \mathbf{x}) + f_2(t, \mathbf{x}), \quad (5)$$

where, t is the independent variable and \mathbf{x} the parameter vector ($\mathbf{x} = [x_1, x_2, x_3, x_4, x_5, x_6, x_7]$).

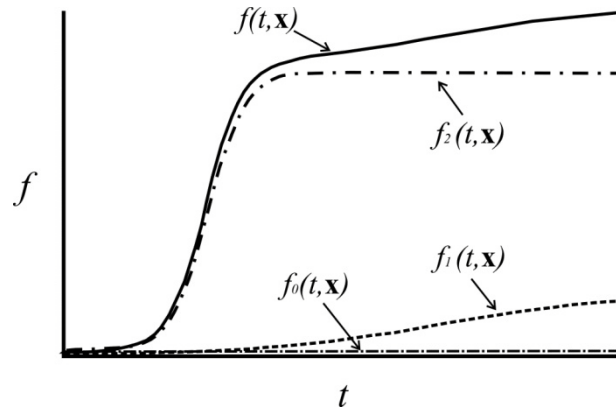


Figure 8. Model function

The first term $f_0(t, \mathbf{x})$ is the lower asymptote, the second and third ones are logistic curves, whose parameterization allows the generation of a model of the VC curve, where t is the expired volume and f is the concentration of CO_2 . This model considers the well known asymmetry of the wave shape.

Terms of Equation (5) are defined in Equations (6).

$$\begin{aligned} f_0(t, \mathbf{x}) &= x_1; \\ f_1(t, \mathbf{x}) &= \frac{(x_2 - x_1)x_3}{1 + e^{(-t-x_4)/x_5}}; \\ f_2(t, \mathbf{x}) &= \frac{(x_2 - x_1)(1 - x_3)}{1 + e^{(-t-x_6)/x_7}}. \end{aligned} \quad (2)$$

The parameters of the Equations (6) are optimized by the Levenberg-Marquardt algorithm [10].

Appendix B

Fuzzy inference is a computer paradigm based on fuzzy set theory, fuzzy if-then rules and fuzzy reasoning.

The structure of fuzzy inference system consists of:

- a rule base which selects the set of fuzzy rules;
- a database (or dictionary) which defines the membership functions used in the fuzzy rules;
- a reasoning mechanism which performs the inference procedure (it derives a conclusion from facts and rules).

The goal of a Takagi-Sugeno Fuzzy Model (TS) [8] is the generation of fuzzy rules from a given input-output data set.

A TS fuzzy rule for a 2 input system takes the form:

$$\text{“If } x \text{ is } A \text{ and } y \text{ is } B \text{ then } z = f(x, y)\text{”}$$

where A and B are fuzzy sets in the antecedent, while $z = f(x, y)$ is a crisp function in the consequent. $f(.,.)$ is very often a polynomial function of x and y .

If $f(.,.)$ is a first order polynomial (a linear function), then the resulting fuzzy inference is called a first order Sugeno fuzzy model. This is the model used in this work.

The rule base is generated starting from an appropriate partition of the input-output data space.

In the input space partitioning, the antecedent of a fuzzy rule defines a local fuzzy region. The consequent describes the local behavior within the fuzzy region.

In this work, both grid partition and subtractive clustering partition were used [6].

In the grid partition, each region is included in a square area (hypercube).

In the cluster partition, each region is determined by covering a subset of the whole input space that characterizes a region of possible occurrence of the input vectors.

The overall output is obtained by aggregation of the rules outputs. Usually, the weighted average is used to perform this operation.

The weighted average expression includes the membership functions in the antecedents and the mathematical expressions of the consequents with their respective parameters. These parameters could be optimized using the input-output data.

References:

1. Abbod M. F., Keyserlingk D. G. v., Linkens D. A., Mahfouf M., 2001, *Survey of utilisation of fuzzy technology in medicine and healthcare*, Fuzzy Sets Syst., 120, 2, pp. 331-349.
2. Crawford A. B., Makowska M., Paiva M., Engel L. A., 1985, *Convection- and diffusion-dependent ventilation maldistribution in normal subjects*, J. Appl. Physiol., 59, 3, pp. 838-46.
3. Fletcher R., Jonson B., Cumming G., Brew J., 1981, *The concept of deadspace with special reference to the single breath test for carbon dioxide*, Br. J. Anaesth., 53, 1, pp. 77-88.
4. Fowler W. S., 1948, *Lung function studies; the respiratory dead space*, Am. J. Physiol., 154, 3, pp. 405-16.
5. Jang J., 1993, *ANFIS: adaptive-network-based fuzzy inference systems*, IEEE Trans. Syst. Man. Cybern., 23, 3, pp. 665-85.
6. Jang J., Gulley N., 2000, *Fuzzy Logic Toolbox: User's Guide*, The Math Works, Inc, Natick, MA, USA.
7. Kline J. A., Kubin A. K., Patel M. M., Easton E. J., Seupal R. A., 2000, *Alveolar dead space as a predictor of severity of pulmonary embolism*, Acad. Emerg. Med., 7, 6, pp. 611-7.
8. Takagi T., Sugeno M., 1985, *Fuzzy identification of systems and its applications to modeling and control.*, IEEE Trans. Syst. Man. Cybern., 15, pp. 116-32.
9. Tang Y., Turner M. J., Baker A. B., 2005, *Effects of alveolar dead-space, shunt and V/Q distribution on respiratory dead-space measurements*, Br. J. Anaesth., 95, 4, pp. 538-48.
10. Tusman G., Scandurra A., Bohm S. H., Suarez-Sipmann F., Clara F., 2009, *Model fitting of volumetric capnograms improves calculations of airway dead space and slope of phase III*, J. Clin. Monit. Comput., 23, 4, pp. 197-206.
11. Wolff G., Brunner J. X., Weibel W., Bowes C. L., Muchenberger R., Bertschmann W., 1989, *Anatomical and series dead space volume: concept and measurement in clinical praxis.*, Appl. Cardiopulm. Pathophysiol., 2, pp. 299-307.
12. Yager R., Filev D., 1994, *Generation of fuzzy rules by mountain clustering*, J. Intell. Fuzzy. Syst., 2, pp. 209-19.
13. Ying H., 1998, *General SISO Takagi-Sugeno fuzzy systems with linear rule consequent are universal approximators*, IEEE Trans. on Fuzzy Systems, 6, 4, pp. 582-7.